Exosomal miR-152-5p/ARHGAP6/ROCK axis regulates apoptosis and fibrosis in cardiomyocytes

SHAOYUAN CHEN[1,2*], YULANG HUANG[3*], RONGZHI LIU[1*], ZIXIANG LIN[1], BIHAN HUANG[1], WEN AI[1,2], JIANJUN HE[4], YULAN GAO[1] and PEIYI XIE[1]

[1]Department of Cardiology, Huazhong University of Science and Technology Union Shenzhen Hospital, Shenzhen, Guangdong 518052; [2]Department of Cardiology, The 6th Affiliated Hospital of Shenzhen University Health Science Center, Shenzhen, Guangdong 518060; [3]Department of Cardiology, Shenzhen Qianhai Shekou Free Trade Zone Hospital, Shenzhen, Guangdong 518067; [4]First Clinical Department, Guangdong Medical University, Zhanjiang, Guangdong 524002, P.R. China

Received November 2, 2022; Accepted February 8, 2023

DOI: 10.3892/etm.2023.11864

Abstract. Acute myocardial infarction (AMI) is a fatal cardiovascular disease with a high mortality rate. The discovery of effective biomarkers is crucial for the diagnosis and treatment of AMI. In the present study, miRNA sequencing and reverse transcription-quantitative polymerase chain reaction techniques revealed that the expression of exosome derived miR-152-5p was significantly downregulated in patients with AMI compared with healthy controls. A series of functional validation experiments were then performed using H9c2 cardiomyocytes. Following transfection of the cardiomyocytes using an miR-152-5p inhibitor, immunofluorescence staining of a-smooth muscle actin revealed a marked increase in fibrosis. Western blotting revealed that the expression levels of the apoptotic protein Bax, TNF-α and collagen-associated proteins were significantly increased, whereas those of the apoptosis-inhibiting factor Bcl-2 and vascular endothelial growth factor A were significantly decreased. Furthermore, the binding of Rho GTPase-activating protein 6 (ARHGAP6) to miR-152-5p was predicted using an online database and verified using a dual-luciferase reporter gene assay. The transfection of cardiomyocytes with miR-152-5p mimics was found to inhibit the activation of ARHGAP6 and Rho-associated coiled-coil containing kinase 2 (ROCK2). These results suggest that miR-152-5p targets ARHGAP6 through the ROCK signaling pathway to inhibit AMI, which implies that miR-152-5p may be a diagnostic indicator and potential target for treatment of myocardial infarction.

Correspondence to: Dr Shaoyuan Chen, Department of Cardiology, Huazhong University of Science and Technology Union Shenzhen Hospital, 89 Taoyuan Road, Nanshan, Shenzhen, Guangdong 518052, P.R. China
E-mail: moter2002@126.com

*Contributed equally

Key words: acute myocardial infarction, miR-152-5p, ROCK signaling pathway, ARHGAP6, cardiomyocyte apoptosis

Introduction

Acute myocardial infarction (AMI) is a severe cardiovascular disease which is caused by acute sustained ischemia and inadequate oxygen supply of the coronary arteries, and results in severe cardiac failure (1). It has a high mortality rate and is a considerable socioeconomic concern (2). AMI is mainly caused by coronary artery occlusion and the interruption of blood flow, leading to ischemic necrosis and irreversible cardiomyocyte loss through oxidative stress, inflammatory responses and morphological changes in myocardial fibroblasts (3-5). Cardiomyocyte loss comprises the necrosis or apoptosis of cardiomyocytes. The loss of cardiomyocyte excitation and contractility leads to functional disorders of cardiomyocyte function. Although persistent myocardial damage can be mitigated by current therapeutic approaches, including surgical intervention, thrombolysis and interventional therapy, it is not possible to alleviate the early massive myocardial cell loss. Due to limited regenerative capacity of cardiomyocytes, the early identification of AMI and the development of effective treatments to reduce cardiomyocyte loss are of great value (6,7).

Clinicians diagnose AMI primarily on the basis of clinical symptoms, electrocardiogram results and serum biomarkers. Traditional serum biomarkers, which include creatine kinase isoenzyme MB (CK-MB) and troponin I/T, present with a lag and may give false-positive results (8). Therefore, it is necessary to develop new biomarkers for the diagnosis of AMI. Exosomes are 30-100 nm bilayer vesicles that carry cellular products such as proteins, mRNA, miRNA and lipids (9,10). MicroRNAs (miRNAs, miRs) from plasma exosomes have been reported to be ideal biomarkers for the early identification of cardiovascular disease and to have great potential for therapeutic and other applications (11,12). There is evidence to suggest that a series of important physiological processes, including the survival, proliferation and angiogenesis of cardiomyocytes are regulated by miRNAs (13,14). In addition, miRNAs have been

shown to stimulate cardiomyocyte proliferation and promote cardiac repair (15,16). For example, Wang *et al* (17) showed that plasma biomarkers miRNA-499 and miRNA-22 have high sensitivity and specificity for the diagnosis of AMI. In another study, 18 exosomal miRNAs were identified to be differentially expressed in patients with AMI compared with patients with coronary artery disease and healthy controls, indicating that these exosomal miRNAs may have the potential be developed as highly sensitive, noninvasive biomarkers for early AMI diagnosis (18). miR-152 is abnormally expressed in a variety of diseases; for example, miR-152-5p has been demonstrated to be a tumor suppressor in gastric cancer (19).

A previous study showed that miR-152-5p is a potential biomarker for myocardial infarction (20). The Ras homolog family member A (RhoA)/Rho-associated protein kinase (ROCK) pathway interacts with numerous other signaling pathways, including the MAPK, hypoxia-inducible factor-1 and NF-κB pathways (21-23). Furthermore, our previous study showed that ROCK is activated in the plasma of patients with acute coronary syndrome (24). The RhoA/ROCK pathway is involved in the regulation of a number of cellular functions, including cell differentiation, gene expression, apoptosis and inflammation. In addition, the inhibition of ROCK decreases cardiac fibrosis and the chemotaxis of inflammatory cytokines (25,26).

Therefore, high-throughput sequencing was performed in the present study to explore the profiles of circulating exosome-derived miRNAs in blood samples from patients with AMI compared with those in healthy individuals. The study further aimed to reveal the regulatory role of miRNAs in AMI.

Materials and methods

Sample collection. Seven patients with AMI (3 male and 4 female, aged between 47 and 69 years, with an average age of 60 years) admitted to Shenzhen Nanshan People's Hospital (Guangdong, China) from October 25 to November 12, 2019 were included in the study, and 9 healthy individuals (5 male and 4 female, aged between 34 and 53 years, with an average age of 43 years) were selected as the control group. Inclusion criteria for AMI: type I myocardial infarction conforming to the global definition and classification of 2018 ESC myocardial infarction, and the onset time of AMI is within 14 days. Inclusion criteria of healthy people: those without hypertension, diabetes, hyperlipidemia, coronary heart disease, and those CT examination with normal coronary artery. Both groups excluded creatinine clearance rate<30 ml/min, liver dysfunction child B, C, infection, trauma or surgical history within 4 weeks, malignant tumors, systemic immune diseases, and the use of steroids, anti-inflammatory and analgesic drugs, immunosuppressants. The study was undertaken with the informed consent of each participant, and all participants signed an informed consent form. A venous blood sample (5 ml) was collected, and sodium citrate was added to prevent coagulation. The blood samples were cryopreserved at -20˚C until further use. All procedures were ethically guided by the principles of the 1964 Declaration of Helsinki and its 2013 amendment.

Exosome isolation and detection. The clinical venous blood samples were thawed on ice, and exosomes were extracted from the blood plasma using exoQuick-TC precipitation (System Biosciences). In brief, ExoQuick-TC was added to the plasma after mixing at 4˚C overnight. Following centrifuge the mixture at 12,000 g, 4˚C for 20 min to remove the supernatant, and the white pellet at the bottom of the centrifuge tube was collected. The biological morphology of exosome was observed by negative staining of transmission electron microscope. In brief, fix purified exosomes with of 2% Paraformaldehyde (PFA) for 5 min at room temperature. The extracted exosomes were diluted 1:20, and then 10 μl was added to a copper net under electron microscope and heated in an oven at 65˚C for 30 min. After drying, the exosomes were labelled with 1% uranyl acetate for 10 min under room temperature. The size and characteristics of the exosomes were observed under a transmission electron microscope (Tecnai G2 Spirit BioTWIN; FEI Company).

RNA extraction. Extraction of total RNA from plasma exosomes and cells was performed using TRIzol® (Invitrogen; Thermo Fisher Scientific, Inc.). Notably, each sample was supplemented with 1 μg glycogen following the addition of isopropyl alcohol. The concentration and integrity of the obtained RNA was determined using a NanoDrop™ 2000 (Thermo Fisher Scientific, Inc.), agarose gel electrophoresis and Bioanalyzer 2100 (Agilent Technologies, Inc.). RNA that had been quality-checked satisfactorily was stored at -80˚C for further study.

miRNA sequencing. An miRNA library was generated with a QIAseq miRNA Library Kit (Qiagen GmbH, cat. no. 331505), and miRNA sequencing was performed using the Illumina HiSeq 2500 System (Illumina, Inc.) after quality control (total RNA is >0.05 ug) by nanodrop 2000 (Thermo Fisher), with an paired-end 50 bp sequencing strategy. Following assessment of the quality of the raw data using FastQC (https://github.com/s-andrews/FastQC), Cutadapt software (cutadapt version 1.15, Marcel Martin) was used to remove the adapters and filter the reads with a length of <17 nucleotides and a percentage of N bases >10%. The calculated transcripts per million values were used as normalized data and read counts <10 were considered unexpressed. After determining the fold change (FC) values, the miRNAs with |log2FC|>1 and false discovery rate <0.01 were considered differentially expressed. Of these, the miRNAs with logFC >1 were upregulated, while those with logFC <-1 were downregulated.

Reverse transcription-quantitative polymerase chain reaction (RT-qPCR) assay. Total RNA was synthesized into cDNA using the EntiLink™ 1st Strand cDNA Synthesis Kit (ELK Biotechnology). Then qPCR amplifications were performed using a EnTurbo™ SYBR Green PCR SuperMix Kit (ELK Biotechnology) with a QuantStudio™ 6 Flex system PCR instrument (Thermo Fisher Scientific, Inc.) under the following thermocycling conditions: 95˚C (30 sec), 95˚C (10 sec), 58˚C (30 sec) and 72˚C (30 sec) for 40 cycles. All experiments were performed in triplicate. Relative gene expression was calculated using the $2^{-\Delta\Delta Cq}$ method (1), with U6 as the reference

Table I. Primer sequences.

Name	Sequence (5'-3')
U6-RT	AACGCTTCACGAATTTGCGT
U6-F	CGCTTCGGCAGCACATATACT
U6-R	AACGCTTCACGAATTTGCGT
rno-miR-152-5p-RT	CTCAACTGGTGTCGTGGAGTCGGCAATTCAGTTGAGAGTCGGAG
rno-miR-152-5p-F	CGGAGGTTCTGTGATACACTCC
rno-miR-152-5p-R	CTCAACTGGTGTCGTGGAGTC
GAPDH-F	AACAGCAACTCCCATTCTTCC
GAPDH-R	TGGTCCAGGGTTTCTTACTCC
ARHGAP6-F	CTCCACAGTAAGCCGACTCAAT
ARHGAP6-R	CAGTGGGACTTCGTAGTCAAAGT
hsa-miR-152-5p-RT	CTCAACTGGTGTCGTGGAGTCGCCAATTCAGTTGAGAGTCCGAG
hsa-miR-152-5p-F	GGCCGGTTCTGTGATACACT
hsa-miR-152-5p-R	GCGACGAGCAAAAAGCTTGT

RT, reverse transcription; F, forward; R, reverse; rno, *Rattus norvegicus*; miR, microRNA; ARHGAP6, Rho GTPase-activating protein 6.

gene for miR-152-5p and GAPDH as the reference gene for ARHGAP6. Primer sequences are shown in Table I.

Bioinformatics. Genes targeted by differentially expressed miRNAs were predicted with the use of a public miRTarBase database (https://mirtarbase.cuhk.edu.cn/~miRTarBase/miRTarBase_2022/php/index.php), and categorized according to their Gene Ontology (GO) terms, which can provide comprehensive information on gene function using topGO (version 2.18.0) software with Fisher's exact test. Pathway identification was performed with KOBAS 2.0 software and hypergeometric tests via the Kyoto Encyclopedia of Genes and Genomes (KEGG) database (https://www.genome.jp/kegg/). Use miRDB database (mirdb.org/) to predict the binding site of miR-152-5p.

Cell culture and transfection. H9c2 rat cardiomyocytes were obtained from the Cell Bank of Type Culture Collection of the Chinese Academy of Sciences (cat. no. GNR 5). The H9c2 cardiomyocytes were cultured in DMEM (Hyclone; Cytiva) containing 10% fetal bovine serum (Invitrogen; Thermo Fisher Scientific, Inc.) in a humidified incubator at 37˚C with 5% CO_2. The H9c2 cardiomyocytes were transfected with 50 nM mimic negative control (NC), sense, 5'-UUUGUACUACACAAAGUACUG-3' and antisense, 3'-AAACAUGAUGUGUUUUCAUGAC-5'; miR-152-5p mimic, sense, 5'-AGGUUCUGUGAUACACUCCGACU-3' and antisense, 3'-UCCAAGACACUAUGUGAGGCUGA-5'; inhibitor NC 5'-CAGUACUUUUGUGUAGUACAAA-3' and miR-152-5p inhibitor, 5'-AGUCGGAGUGUAUCACAGAACCU-3' using Lipofectamine® 2000 (Invitrogen; Thermo Fisher Scientific, Inc.) at 37˚C. After 6 h of transfection, the solution was replaced with cell culture medium. Cells were cultured for another 48 h prior to analysis by RT-qPCR. Accordingly, four groups were established for the experiment: Mimic NC, miR-152-5p mimic, inhibitor NC and miR-152-5p inhibitor. The miR-152-5p mimic, inhibitor and their NCs were synthesized by Guangzhou RiboBio Co., Ltd.

Western blot analysis. H9c2 cardiomyocytes were lysed in cold radioimmunoprecipitation assay lysis buffer (Fermentas; Thermo Fisher Scientific, Inc.). The concentration of the extracted protein was determined using a BCA Protein Quantification Kit (AS1086; Aspen Biotechnology). A total of 50 μg protein was loaded per lane. Proteins were then separated by 12% SDS-PAGE and transferred to polyvinylidene difluoride membranes (MilliporeSigma), followed by the addition of Tris-buffered saline and 0.1% Tween 20 (ASPEN) containing 5% skimmed milk (BD Biosciences) for 1 h at room temperature to block the membranes. Subsequently, the membranes were incubated with primary antibodies overnight at 4˚C (Table SI). Then, the membranes were then washed thoroughly three times with phosphate-buffered saline containing 0.1% Tween-20 (PBST) and then incubated with goat anti-rabbit secondary antibodies (1:10,000; Abcam) for 1 h at room temperature. After washing three times with PBST, chemiluminescence detection was performed with ECL chemiluminescence detection kit (ASPEN). Relative protein expression was analyzed with Image-Pro Plus software 6.0 (Media Cybernetics, Inc.) and normalized to GAPDH.

Immunofluorescence analysis. Cells were fixed with 4% paraformaldehyde for 30 min at room temperature and then endogenous peroxidase/phosphatase activity was blocked with 3% H_2O_2 for 20 min in a dark environment. The cells were then incubated with an anti-α-smooth muscle actin (α-SMA) antibody (1:200, 55135-1-AP; ProteinTech Group, Inc.) at a dilution of 1:1,000 with 5% BSA (Roche) and incubated overnight in a humidified box at 4˚C. Cy3-labeled fluorescent secondary antibody (AS1109; ASPEN Biotechnology) was added at a dilution of 1:100 after washing, and incubated for 50 min at room temperature. Then, the cells were washed three times with 1X PBS, and counterstained with DAPI (AS1075; ASPEN Biotechnology) for 5 min at room temperature. Confocal microscopy was performed and fluorescence was analysed using a fluorescence microscope (Leica DMI4000B; Leica Microsystems, Inc.).

Dual-luciferase reporter assay. The full-length 3' untranslated region (3'UTR) amplification products of the Rho GTPase-activating protein 6 (ARHGAP6) gene containing the binding sites of miR-152-5p predicted by the miRDB database were transferred into a pmiRGLO expression vector (Tsingke Biotechnology) to form ARHGAP6-wild-type (WT). Independently, a site-specific mutation targeting the predicted binding site for miR-152-5p in the ARHGAP6 gene was established, and the resultant mutant sequence was also introduced into a pmiRGLO expression vector to form ARHGAP6-MUT. Then, the H9c2 cardiomyocytes were co-transfected with a reporter plasmid and a miR-152-5p mimic or mimic-NC using Lipofectamine 2000. The ARHGAP6-WT- and ARHGAP6-MUT-transfected cells were each used to establish a blank control, miR-152-5p mimic and mimic-NC group with three duplicate wells in each group. After 48 h of culture, the luciferase activity of the cells was detected using a fluorescence microplate reader (Spark 10M; Tecan Group, Ltd.) according to the instructions of the Dual Luciferase Reporter Gene Assay Kit (RG008, Beyotime). The relative luciferase activity was calculated using the following equation: Relative luciferase activity=firefly luciferase activity value/Renilla luciferase activity value.

Statistical analysis. Statistical analysis and visualization were performed with SPSS software (version 26; IBM Corp.) and GraphPad (version 8.0.2; GraphPad Software, Inc.), respectively. Data are presented as the mean ± SD. Data were analyzed for significance using the nonparametric Mann-Whitney U test. $P<0.05$ was considered to indicate a statistically significant difference. All experiment was repeated three times.

Results

miR-152-5p is significantly downregulated in patients with AMI. Exosomes were extracted from the peripheral blood samples of 7 patients with AMI and 9 healthy individuals (Fig. 1). RNA was extracted from the exosomes for miRNA sequencing. The different expression miRNA profiles of the two groups are shown in Fig. 2A. There were 544 upregulated and 518 downregulated miRNAs, of which miR-152-5p was the most significantly downregulated (Table II). Therefore, an in-depth analysis of miR-152-5p was performed. First, the expression of miR-152-5p in the venous blood exosomes of patients with AMI and healthy individuals was detected by RT-qPCR. The results confirmed that miR-152-5p was significantly reduced in the serum of the patients with AMI compared with the healthy controls (Fig. 2B), which was consistent with the sequencing results and illustrated the accuracy of the sequencing data. GO analysis showed that various terms, including 'cell', 'cell part', 'protein geranylgeranyl transferase activity' and 'transcription elongation from RNA polymerase I promoter' were enriched in AMI. The results of KEGG analysis shows the pathways that were enriched with the target genes of miR-152-5p, as predicted using the miRDB database (Fig. 2C and D).

miR-152-5p inhibits cardiomyocyte apoptosis and fibrosis. Considering the results of the differential expression analysis, we hypothesized that miR-152-5p may be involved in associated biological functions in the cardiomyocytes of patients with AMI. Therefore, miR-152-5p mimic and miR-152-5p inhibitor were transfected into H9c2 cardiomyocytes to explore the effects of miR-152-5p on markers of cardiomyocyte apoptosis and fibrosis. Immunofluorescence analysis revealed that α-SMA staining was significantly reduced after transfection of the miR-152-5p mimic compared with mimic NC, indicating that the miR-152-5p mimic significantly reduces H9c2 cardiomyocyte fibrosis (Fig. 3A). In addition, transfection with the miR-152-5p inhibitor resulted in increased α-SMA staining compared to transfection with the inhibitor NC (Fig. 3A). Following the transfection of cardiomyocytes with the miR-152-5p mimic, western blotting revealed a significant reduction in the expression of the proapoptotic protein Bax and the proinflammatory cytokine TNF-α (Fig. 3B and C), while the expression of Bcl-2, an antiapoptotic protein, was significantly increased. By contrast, these effects were reversed following transfection with miR-152-5p inhibitor; specifically, the expression levels of Bax and TNF-αwere significantly increased, but the expression level of Bcl-2 was significantly decreased (Fig. 3B and C).

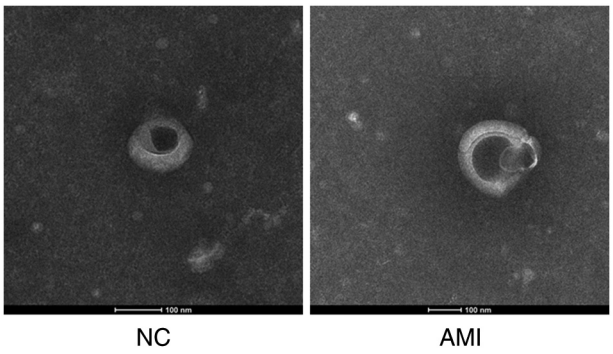

Figure 1. Transmission electron microscopy images of exosomes. NC, normal control; AMI, acute myocardial infarction.

Immunofluorescence was used to detect the level of cardiomyocyte fibrosis, and the results revealed that α-SMA staining was markedly reduced after transfection with miR-152-5p mimic compared with mimic NC, whereas transfection with miR-152-5p inhibitor resulted in an increase in α-SMA staining. These results indicate that the miR-152-5p mimic reduced H9c2 cardiomyocyte fibrosis (Fig. 4A). Furthermore, the detection of cardiomyocyte fibrosis-associated protein markers using western blotting revealed that the miR-152-5p mimic decreased the expression of collagen I, collagen III and angiotensin II compared with the mimic-NC (Fig. 4B). Together these findings suggest that miR-152-5p expression suppresses fibrosis in cardiomyocytes. Moreover, the increased expression of vascular endothelial growth factor A (VEGFA) in the miR-152-5p mimic group compared with the mimic-NC group indicated that miR-152-5p promoted the regeneration of cardiomyocytes (Fig. 4B).

miR-152-5p inhibits the ROCK signaling pathway. The ROCK signaling pathway plays an important role in the occurrence and development of cardiovascular diseases via the regulation of cardiomyocyte apoptosis, fibrosis, inflammation and cardiac remodeling, and phosphorylation is a key factor in the

Table II. Top 10 most significantly downregulated miRNAs.

miRNA	log_2(FC)	P-value	FDR
hsa-miR-152-5p	-7.53	$5.77x10^{-84}$	$1.48x10^{-80}$
hsa-miR-3622a-5p	-6.34	$3.57x10^{-65}$	$3.05x10^{-62}$
hsa-miR-631	-6.35	$1.89x10^{-63}$	$1.22x10^{-60}$
hsa-miR-3940-3p	-7.42	$2.64x10^{-53}$	$9.68x10^{-51}$
hsa-miR-584-3p	-5.77	$1.10x10^{-49}$	$3.54x10^{-47}$
hsa-miR-4258	-6.16	$6.13x10^{-49}$	$1.58x10^{-46}$
hsa-miR-3192-5p	-5.51	$1.08x10^{-48}$	$2.53x10^{-46}$
hsa-miR-3146	-5.22	$1.86x10^{-48}$	$3.98x10^{-46}$
hsa-miR-6731-5p	-5.40	$2.83x10^{-48}$	$5.50x10^{-46}$
hsa-miR-6505-5p	-5.16	$3.00x10^{-48}$	$5.50x10^{-46}$

miRNA/miR, microRNA; log_2(FC), log_2(fold change); FDR, false discovery rate; hsa, *homo sapiens*.

function of ROCK (26). Therefore, the effect of miR-152-5p on the ROCK signaling pathway in cardiomyocytes was investigated. As shown in Fig. 5, transfection with the miR-152-5p mimic significantly decreased the expression of ROCK2 and the level of phosphorylated (p-)ROCK compared with those in the mimic-NC group; by contrast, the miR-152-5p inhibitor significantly increased ROCK2 and p-ROCK2 levels compared with those in the inhibitor-NC group. However, the ratio of p-ROCK2 to total ROCK2 in the cardiomyocytes was unchanged regardless of transfection with miR-152-5p mimic or inhibitor. The obtained results indicate that inhibition of miR-152-5p expression attenuated the inhibitory effect of miR-152-5p on the ROCK signaling pathway.

ARHGAP6 is a target gene of miR-152-5p. To further explore the mechanism underlying the effects of the ROCK signaling pathway in cardiomyocytes, target gene prediction for miR-152-5p was performed using the miRDB database. A total of 93 target genes were predicted to bind with miR-152-5p. A review of the literature indicated that ARHGAP6, a member of the Rho GTPase family, is closely associated with the ROCK signaling pathway and that ARHGAP6 is upstream of ROCK (27). Therefore, a series of experiments on ARHGAP6 were performed. First, the binding sites between miR-152-5p and the 3'UTR of ARHGAP6 were predicted (Fig. 6A). Then, luciferase reporter constructs containing the ARHGAP6 3'UTR with or without a miR-152-5p binding site mutant sequence were generated and the luciferase activities of the H9c2 cells were evaluated following co-transfection with a vector expressing miR-152-5p. In the ARHGAP6-WT cells, co-transfection with miR-152-5p significantly inhibited the luciferase activity of the ARHGAP6 gene compared with that in the NC mimic group (Fig. 6B). However, in ARHGAP6-MUT cells, the transfection of miR-152-5p had no significant effect on the luciferase activity of the ARHGAP6 gene (Fig. 6B). These results indicate that miR-152-5p regulated the expression of the ARHGAP6 gene by targeting its 3'UTR. Furthermore, RT-qPCR analysis showed that the mRNA expression level of ARHGAP6 was significantly reduced in the miR-152-5p mimic group and increased in the miR-152-5p inhibitor group compared with that in the respective NC group (Fig. 6C). In summary, the present study suggests that miR-152-5p inhibited the ROCK signaling pathway, apoptosis and fibrosis in cardiomyocytes via the targeting of ARHGAP6.

Discussion

In the present study, 544 upregulated and 518 downregulated miRNAs were identified in the plasma exosomes of patients with AMI; among these, miR-152-5p was the most strongly downregulated. Previous studies have shown that miR-152 may promote neonatal cardiomyocyte proliferation (15). This was supported by the results of the present study, which indicate that increased miR-152-5p expression promoted the expression of VEGFA. AMI injury is mainly manifested as damage to cardiomyocytes. Consequently, the present study focused on the effect of miR-152-5p on H9c2 cardiomyocytes and its potential mechanism. In a previous study using HepG2 and MHCC97 cells, miR-152-5p overexpression activated apoptosis-associated factors and upregulated the expression of forkhead box class O via the JNK pathway (28). Furthermore, Zong *et al* (29) reported that miR-152-5p participated in cigarette smoke extract-induced human bronchial epithelial cell inflammation by regulating the ERK signaling pathway. These studies suggested that miR-152-5p may promote tumor cell apoptosis and participate in the inflammatory response and other functions in certain cells and diseases. In the present study, it was found that miR-152-5p inhibits the apoptosis and fibrosis of H9c2 cardiomyocytes which indicates that it has the potential to serve a myocardial protective role.

During the process of myocardial infarction, the myocardium undergoes structural changes, such as cardiomyocyte apoptosis, increased expression of extracellular matrix proteins, cardiomyocyte fibrosis and cardiomyocyte hypertrophy (30-32). Studies have shown that miRNAs play important roles in the pathological processes of cardiomyocyte apoptosis, fibrosis and hypertrophy following myocardial infarction. For example, the overexpression of miR-145-5p was demonstrated to inhibit hypoxia/reoxygenation-induced cardiomyocyte apoptosis, alleviate myocardial ischemia/reperfusion injury and exert cardioprotective effects (33). In addition, miRNA-214 was found to be highly expressed in the serum

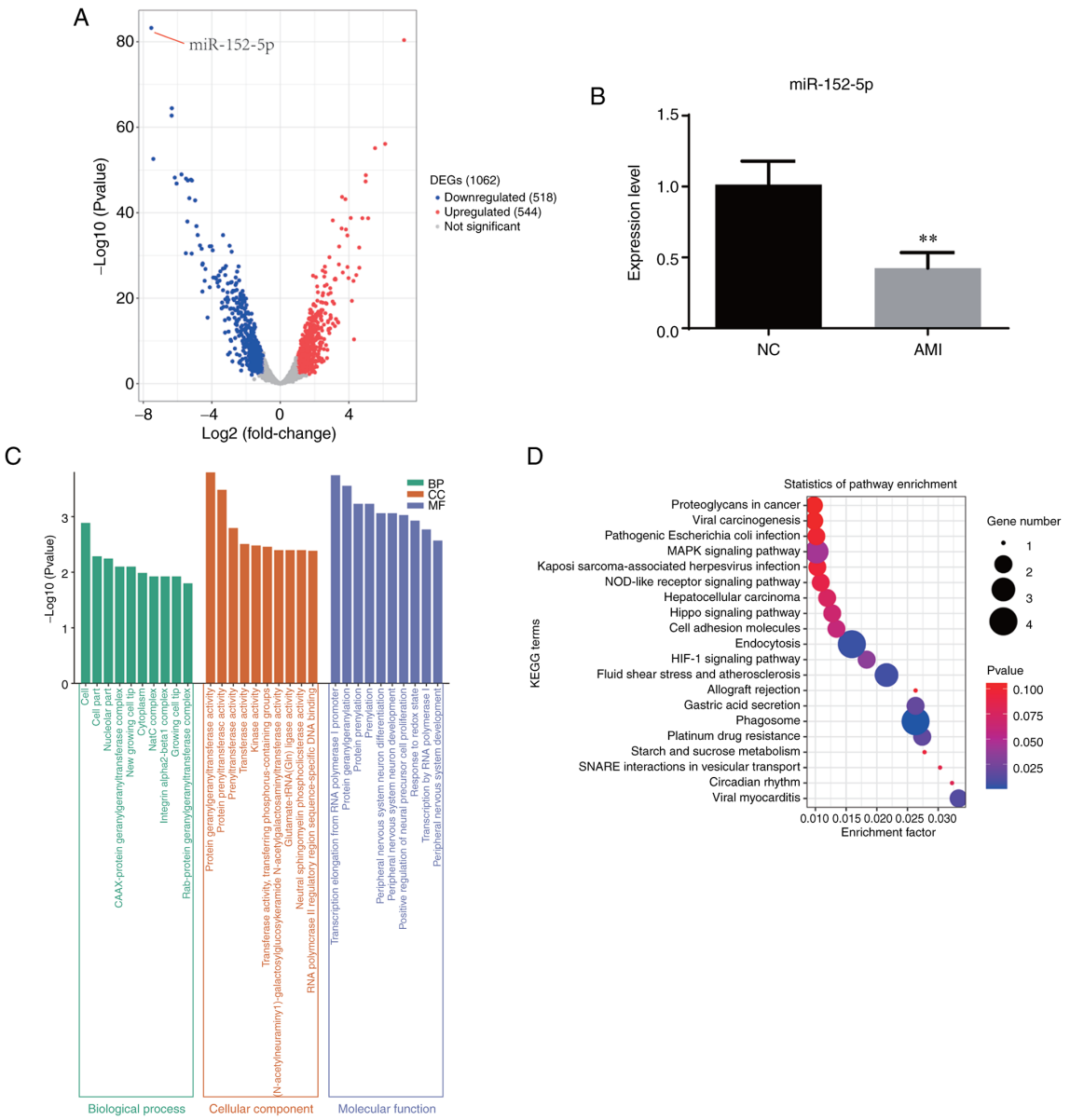

Figure 2. miR-152-5p is significantly downregulated in patients with AMI. (A) Volcano plot based on the differential expression of miRNAs in patients with AMI compared with healthy individuals. Red indicates high expression, and blue indicates low expression. (B) Relative expression levels of miR-152-5p in patients with AMI compared with healthy individuals as verified by reverse transcription-quantitative polymerase chain reaction. (C) Gene Ontology analysis for patients with AMI compared with healthy individuals. (D) KEGG enrichment for patients with AMI compared with healthy individuals. **P<0.01. miR/miRNA, microRNA; AMI, acute myocardial infarction; NC, normal (healthy) controls; DEG, differentially expressed gene; NC, normal (healthy) control; BP, biological process; CC, cellular component; MF, molecular function; KEGG, Kyoto Encyclopedia of Genes and Genomes.

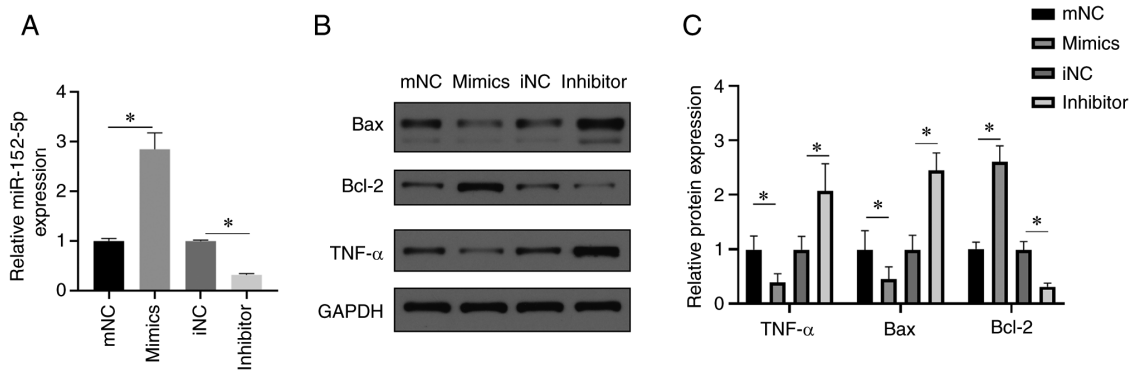

Figure 3. miR-152-5p affects apoptosis markers in H9c2 cells. (A) Transfection efficiency of miR-152-5p mimic and inhibitor. (B) Representative western blotting results for TNF-α, Bax and Bcl-2. (C) Relative expression levels of TNF-α, Bax and Bcl-2. *P<0.05. miR, microRNA; mNC, mimics negative control; mimic, miR-152-5p mimic; iNC, inhibitor NC; inhibitor, miR-152-5p inhibitor.

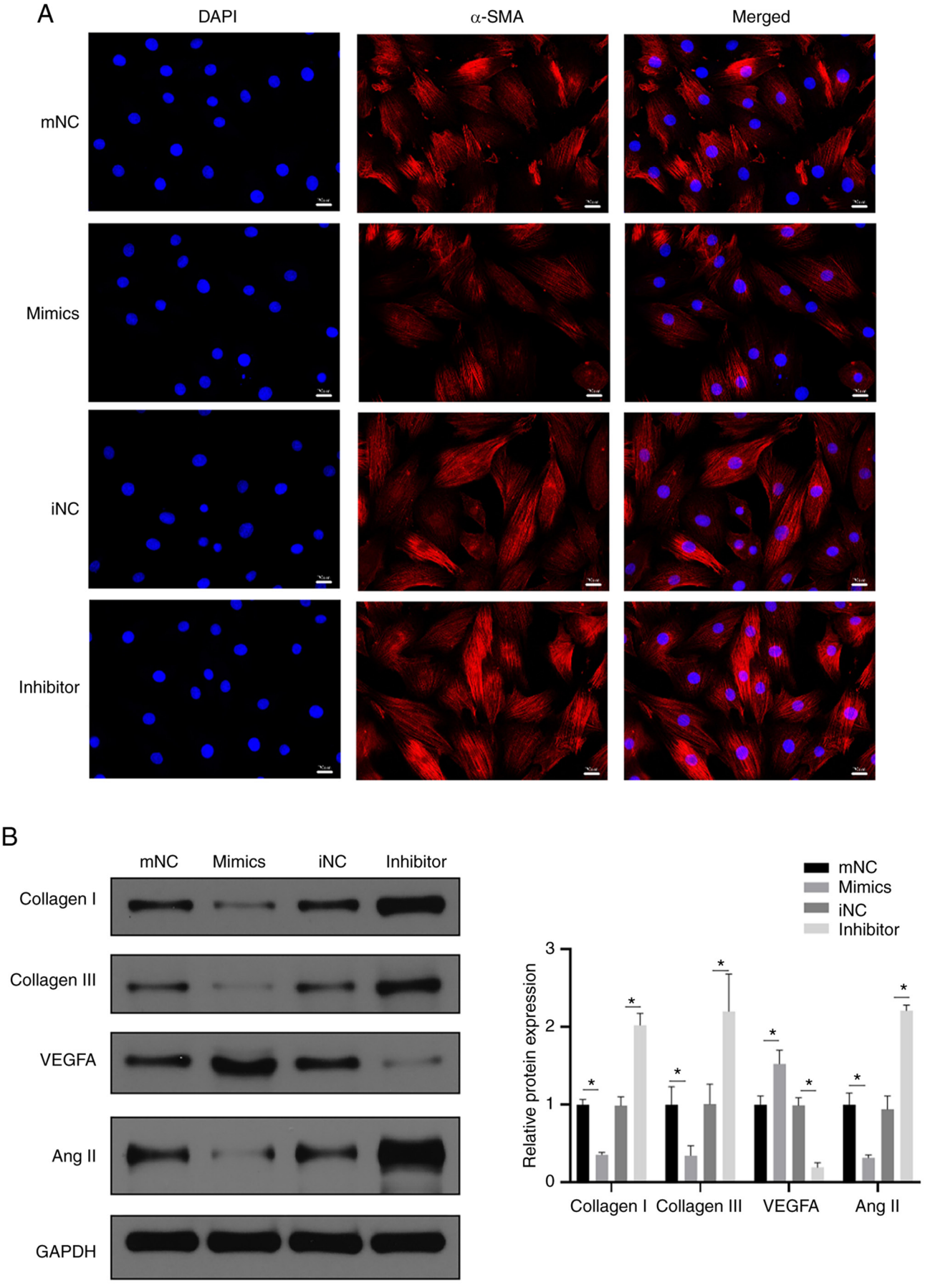

Figure 4. miR-152-5p affects the fibrosis of H9c2 cells. (A) Effect of miR-152-5p on cardiomyocyte fibrosis was evaluated using α-SMA immunofluorescence analysis. Blue represents nuclei and red represents collagen fibers Scale bar, 20 um. (B) Effects of the miR-152-5p mimic or inhibitor on cardiomyocyte fibrosis-associated protein markers. *P<0.05. miR, microRNA; α-SMA, α-smooth muscle actin; VEGFA, vascular endothelial growth factor A; Ang II, angiotensin II; mNC, mimics NC; mimics, miR-152-5p mimics; iNC, inhibitor NC; inhibitor, miR-152-5p inhibitor.

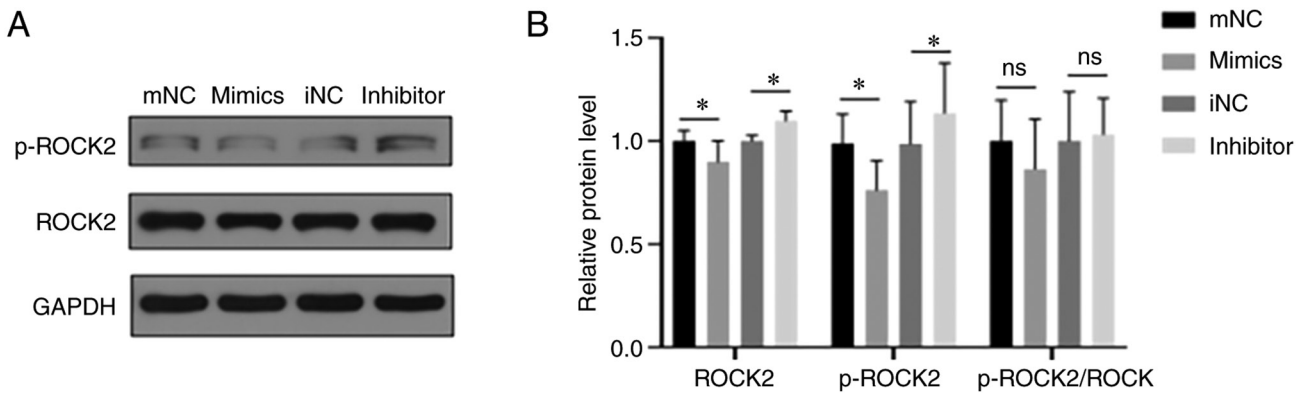

Figure 5. Effects of the miR-152-5p mimic or inhibitor on ROCK signaling. (A) Representative western blots for p-ROCK2 and ROCK2 in transfected cardiomyocytes. (B) Relative levels of p-ROCK2, ROCK2 and p-ROCK2/ROCK2 among the four groups. *P<0.05. ns, not significant; miR, microRNA; ROCK2, Rho-associated coiled-coil containing kinase 2; p-, phosphorylated; mNC, mimics NC; mimics, miR-152-5p mimics; iNC, inhibitor NC; inhibitor, miR-152-5p inhibitor.

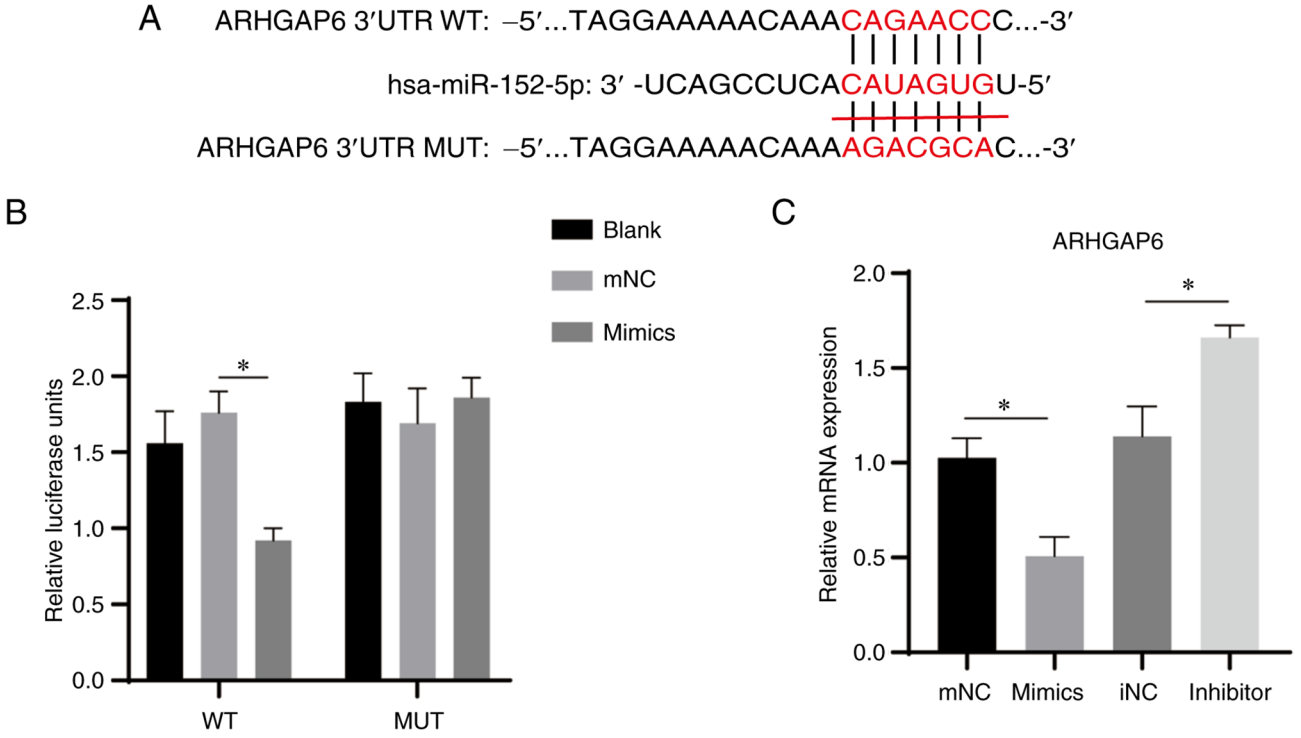

Figure 6. miR-152-5p targets the ARHGAP6 3'UTR. (A) Predicted target sequence for miR-152-5p in the ARHGAP6 3'UTR. (B) Luciferase reporter assays were performed to confirm the binding between miR-152-5p and ARHGAP6. (C) Relative expression level of ARHGAP6 in transfected cardiomyocytes as verified by reverse transcription-quantitative polymerase chain reaction. *P<0.05. miR, microRNA; ARHGAP6, Rho GTPase-activating protein 6; UTR, untranslated region; WT, wild type; MUT, mutant; mNC, mimics NC; mimics, miR-152-5p mimics; iNC, inhibitor NC; inhibitor, miR-152-5p inhibitor.

of elderly patients with AMI, and inhibited the apoptosis of human cardiomyocytes, indicating that miRNA-214 contributes to myocardial infarction (34). Furthermore, the excessive deposition of collagen also causes cardiac dysfunction (35). The results of the present study show that miR-152-5p was downregulated in patients with AMI and the knockdown of miR-152-5p promoted apoptosis and fibrosis in H9c2 cardiomyocytes. By contrast, the increased expression in miR-152-5p reduced the fibrosis of myocardial cells and may promote their regeneration. Therefore, we hypothesize that miR-152-5p plays an important role in the incidence and progression of AMI by inhibiting cardiomyocyte apoptosis and fibrosis.

In the present study, miR-152-5p was shown to inhibit the expression of ROCK2. ARHGAP6, which is upstream of ROCK, was identified to be targeted by miR-152-5p. A number of studies have shown a strong connection between ROCK and the Rho GTPase gene family. The Rho kinases, namely ROCK1 and ROCK2, are important downstream effectors of the Rho GTPases and ARHGAP6 is a member of the Rho GTPase gene family (27,36,37). ROCK1 and ROCK2 are involved in the control of important physiological functions, including migration, proliferation, cell contraction, inflammation and adhesion (38). The expression of ROCK2 in the heart is much higher than that of ROCK1 (39). The interaction between ROCK and

ARHGAP6 has been reported to play a significant role in autosomal dominant polycystic kidney disease, diffuse-type gastric cancer, glaucoma and other diseases (36,40,41). The results of the present study suggest that miR-152-5p may be involved in the ROCK signaling pathway via the targeting of ARHGAP6. Interestingly, the present study found that miR-152-5p decreased both ROCK2 and p-ROCK2 levels, but the ratio of p-ROCK2 to ROCK2 did not change. We hypothesize that miR-152-5p may regulate the expression of ROCK2, but not its activation. ROCK2 has previously been shown to be involved in the activation and aggregation of inflammatory factors, and to aggravate the inflammatory response of endothelial cells after myocardial ischemia injury (42). The pathogenic role of the ROCK signaling pathway in AMI indicates that inhibiting the activity of ROCK may provide a novel therapeutic strategy for AMI. The present study has focused on the effects of miR-152-5p in the regulation of cardiomyocyte fibrosis and apoptosis markers, and preliminary experiments have revealed the possibility that miR-152-5p exerts regulatory effects on cardiomyocytes by targeting ARHGAP6 to affect the ROCK signaling pathway. Therefore, it is speculated that miR-152-5p inhibits apoptosis, inflammatory factor release and myocardial fibrosis by targeting the ARHGAP6/ROCK pathway in cardiomyocytes.

In conclusion, miRNA expression profiles in AMI patients were analyzed, which revealed that the expression of miR-152-5p was downregulated in patients with AMI. Analyses of transfected cardiomyocytes were performed, which suggest that miR-152-5p targets ARHGAP6 through the ROCK signaling pathway to inhibit cardiomyocyte apoptosis, inflammatory factor release and fibrosis, thereby restricting the development of AMI. These results may provide the basis for further exploration of the role of miR-152-5p in the treatment of myocardial infarction. However, the molecular mechanisms of miR-152-5p are likely to involve more complex biological pathways in AMI and require additional in-depth exploration in the future.

Acknowledgements

Not applicable.

Funding

This study was supported by Shenzhen Science and Technology Innovation Commission Fund (reference nos. JCYJ20180302144649363 and JCYJ20220530141815035) and Healthy Science and technology project of Nanshan District (reference nos. NS2022062 and NS2020016).

Availability of data and materials

The raw miRNA data are available in the Zenodo repository (zenodo.org/record/7425965#). The other datasets used and/or analyzed during the current study are available from the corresponding author on reasonable request.

Authors' contributions

SC, YH and RL conceived the study, participated in its design and coordination and helped to draft the manuscript. ZL and BH collected samples, conducted experiments and analyzed the results. WA and JH interpreted data and wrote the manuscript. JH and YG designed and supervised the study. PX participated in research conception and design, and revised and finalized the draft. SC and YG confirm the authenticity of all the raw data. All authors read and approved the final manuscript.

Ethics approval and consent to participate

The study was approved by the Research Ethics Committee of the Shenzhen Nanshan People's Hospital (approval no. 20180211093103602). All procedures conformed with the principles of the 1964 Declaration of Helsinki and its 2013 amendment. The research was conducted with the informed consent of each participant, and all participants signed informed consent forms.

Patient consent for publication

Not applicable.

Competing interests

The authors declare that they have no competing interests.

References

1. Livak KJ and Schmittgen TD: Analysis of relative gene expression data using real-time quantitative PCR and the 2(-Delta Delta C(T)) method. Methods 25: 402-408, 2001.
2. Benjamin EJ, Muntner P, Alonso A, Bittencourt MS, Callaway CW, Carson AP, Chamberlain AM, Chang AR, Cheng S, Das SR, *et al*: Heart disease and stroke statistics-2019 update: A report from the American heart association. Circulation 139: e56-e528, 2019.
3. Bennett S, Ravindran R, Duckett S, Cubukcu A, Jones H and Kwok CS: Acute coronary syndrome secondary to cardiac infiltration and coronary occlusion of chronic lymphocytic leukemia-a case report. J Cardiol Cases 23: 257-260, 2020.
4. Fath AR, Aglan A, Varkoly KS, Eldaly AS, Beladi RN, Forlemu A, Mihyawi N, Solsi A, Israr S and Lucas AR: Distinct coagulopathy with myocardial injury and pulmonary embolism in COVID-19. J Investig Med High Impact Case Rep 9: 23247096211019559, 2021.
5. Zhang X, Shao C, Cheng S, Zhu Y and Liang B: Effect of Guanxin V in animal model of acute myocardial infarction. BMC Complement Med Ther 21: 72, 2021.
6. Galiuto L, DeMaria AN and Iliceto S: Microvascular damage during myocardial ischemia-reperfusion: Pathophysiology, clinical implications and potential therapeutic approach evaluated by myocardial contrast echocardiography. Ital Heart J 1: 108-116, 2000.
7. Li M, Tang X, Liu X, Cui X, Lian M, Zhao M, Peng H and Han X: Targeted miR-21 loaded liposomes for acute myocardial infarction. J Mater Chem B 8: 10384-10391, 2020.
8. Peacock WF, Baumann BM, Rivers EJ, Davis TE, Handy B, Jones CW, Hollander JE, Limkakeng AT, Mehrotra A, Than M, *et al*: Using sex-specific cutoffs for high-sensitivity cardiac troponin T to diagnose acute myocardial infarction. Acad Emerg Med 28: 463-466, 2021.
9. Joyce DP, Kerin MJ and Dwyer RM: Exosome-encapsulated microRNAs as circulating biomarkers for breast cancer. Int J Cancer 139: 1443-1448, 2016.
10. Wang J, Li X, Wu X, Wang Z, Zhang C, Cao G and Yan T: Expression profiling of exosomal miRNAs derived from the peripheral blood of kidney recipients with DGF using high-throughput sequencing. Biomed Res Int 2019: 1759697, 2019.
11. Chen G, Wang M, Ruan Z, Zhu L and Tang C: Mesenchymal stem cell-derived exosomal miR-143-3p suppresses myocardial ischemia-reperfusion injury by regulating autophagy. Life Sci 280: 119742, 2021.

12. Long R, Gao L, Li Y, Li G, Qin P, Wei Z, Li D, Qian C, Li J and Yang G: M2 macrophage-derived exosomes carry miR-1271-5p to alleviate cardiac injury in acute myocardial infarction through down-regulating SOX6. Mol Immunol 136: 26-35, 2021.
13. Aonuma T, Moukette B, Kawaguchi S, Barupala NP, Sepulveda MN, Corr C, Tang Y, Liangpunsakul S, Payne RM, Willis MS and Kim IM: Cardiomyocyte microRNA-150 confers cardiac protection and directly represses proapoptotic small proline-rich protein 1A. JCI Insight 6: e150405, 2021.
14. El Fatimy R, Boulaassafre S, Bouchmaa N, El Khayari A, Vergely C, Malka G and Rochette L: The emerging role of miRNA-132/212 cluster in neurologic and cardiovascular diseases: Neuroprotective role in cells with prolonged longevity. Mech Ageing Dev 199: 111566, 2021.
15. Eulalio A, Mano M, Dal Ferro M, Zentilin L, Sinagra G, Zacchigna S and Giacca M: Functional screening identifies miRNAs inducing cardiac regeneration. Nature 492: 376-381, 2012.
16. Henning RJ: Cardiovascular exosomes and MicroRNAs in cardiovascular physiology and pathophysiology. J Cardiovasc Transl Res 14: 195-212, 2021.
17. Wang X, Tian L and Sun Q: Diagnostic and prognostic value of circulating miRNA-499 and miRNA-22 in acute myocardial infarction. J Clin Lab Anal 34: 2410-2417, 2020.
18. Guo M, Li R, Yang L, Zhu Q, Han M, Chen Z, Ruan F, Yuan Y, Liu Z, Huang B, *et al*: Evaluation of exosomal miRNAs as potential diagnostic biomarkers for acute myocardial infarction using next-generation sequencing. Ann Transl Med 9: 219, 2021.
19. You W, Zhang X, Ji M, Yu Y, Chen C, Xiong Y, Liu Y, Sun Y, Tan C, Zhang H, *et al*: MiR-152-5p as a microRNA passenger strand special functions in human gastric cancer cells. Int J Biol Sci 14: 644-653, 2018.
20. Chen X, Huang F, Liu Y, Liu S and Tan G: Exosomal miR-152-5p and miR-3681-5p function as potential biomarkers for ST-segment elevation myocardial infarction. Clinics (Sao Paulo) 77: 100038, 2022.
21. Pacary E, Tixier E, Coulet F, Roussel S, Petit E and Bernaudin M: Crosstalk between HIF-1 and ROCK pathways in neuronal differentiation of mesenchymal stem cells, neurospheres and in PC12 neurite outgrowth. Mol Cell Neurosci 35: 409-423, 2007.
22. Zhou H, Sun Y, Zhang L, Kang W, Li N and Li Y: The RhoA/ROCK pathway mediates high glucose-induced cardiomyocyte apoptosis via oxidative stress, JNK, and p38MAPK pathways. Diabetes Metab Res Rev 34: e3022, 2018.
23. Huang L, Li Q, Wen R, Yu Z, Li N, Ma L and Feng W: Rho-kinase inhibitor prevents acute injury against transient focal cerebral ischemia by enhancing the expression and function of GABA receptors in rats. Eur J Pharmacol 797: 134-142, 2017.
24. Yang T, Fang F, Chen Y, Ma J, Xiao Z, Zou S, Zheng N, Yan D, Liao S, Chen S, *et al*: Elevated plasma interleukin-37 playing an important role in acute coronary syndrome through suppression of ROCK activation. Oncotarget 8: 9686-9695, 2017.
25. Okamoto R, Li Y, Noma K, Hiroi Y, Liu PY, Taniguchi M, Ito M and Liao JK: FHL2 prevents cardiac hypertrophy in mice with cardiac-specific deletion of ROCK2. FASEB J 27: 1439-1449, 2013.
26. Amin F, Ahmed A, Feroz A, Khaki PSS, Khan MS, Tabrez S, Zaidi SK, Abdulaal WH, Shamsi A, Khan W and Bano B: An update on the association of protein kinases with cardiovascular diseases. Curr Pharm Des 25: 174-183, 2019.
27. Prakash SK, Paylor R, Jenna S, Lamarche-Vane N, Armstrong DL, Xu B, Mancini MA and Zoghbi HY: Functional analysis of ARHGAP6, a novel GTPase-activating protein for RhoA. Hum Mol Genet 9: 477-488, 2000.
28. Chang DL, Wei W, Yu ZP and Qin CK: miR-152-5p inhibits proliferation and induces apoptosis of liver cancer cells by up-regulating FOXO expression. Pharmazie 72: 338-343, 2017.
29. Zong DD, Liu XM, Li JH, Long YJ, Ouyang RY and Chen Y: LncRNA-CCAT1/miR-152-5p is involved in CSE-induced inflammation in HBE cells via regulating ERK signaling pathway. Res Sq, 2021.
30. Duisters RF, Tijsen AJ, Schroen B, Leenders JJ, Lentink V, van der Made I, Herias V, van Leeuwen RE, Schellings MW, Barenbrug P, *et al*: miR-133 and miR-30 regulate connective tissue growth factor: Implications for a role of microRNAs in myocardial matrix remodeling. Circ Res 104: 170-178, 6p, 2009.
31. Chen Y, Zhao Y, Chen W, Xie L, Zhao ZA, Yang J, Chen Y, Lei W and Shen Z: MicroRNA-133 overexpression promotes the therapeutic efficacy of mesenchymal stem cells on acute myocardial infarction. Stem Cell Res Ther 8: 268, 2017.
32. Frangogiannis NG: Cardiac fibrosis. Cardiovasc Res 117: 1450-1488, 2021.
33. Cheng C, Xu DL, Liu XB, Bi SJ and Zhang J: MicroRNA-145-5p inhibits hypoxia/reoxygenation-induced apoptosis in H9c2 cardiomyocytes by targeting ROCK1. Exp Ther Med 22: 796, 2021.
34. Yin Y, Lv L and Wang W: Expression of miRNA-214 in the sera of elderly patients with acute myocardial infarction and its effect on cardiomyocyte apoptosis. Exp Ther Med 17: 4657-4662, 2019.
35. Kurose H: Cardiac fibrosis and fibroblasts. Cells 10: 1716, 2021.
36. Komatsu M, Ichikawa H, Chiwaki F, Sakamoto H, Komatsuzaki R, Asaumi M, Tsunoyama K, Fukagawa T, Matsushita H, Boku N, *et al*: ARHGAP-RhoA signaling provokes homotypic adhesion-triggered cell death of metastasized diffuse-type gastric cancer. Oncogene 41: 4779-4794, 2022.
37. Li Y, Decker S, Yuan ZA, Denbesten PK, Aragon MA, Jordan-Sciutto K, Abrams WR, Huh J, McDonald C, Chen E, *et al*: Effects of sodium fluoride on the actin cytoskeleton of murine ameloblasts. Arch Oral Biol 50: 681-688, 2005.
38. Loirand G: Rho kinases in health and disease: From basic science to translational research. Pharmacol Rev 67: 1074-1095, 2015.
39. Julian L and Olson MF: Rho-associated coiled-coil containing kinases (ROCK): Structure, regulation, and functions. Small GTPases 5: e29846, 2014.
40. Streets AJ, Prosseda PP and Ong AC: Polycystin-1 regulates ARHGAP35-dependent centrosomal RhoA activation and ROCK signaling. JCI Insight 5: e135385, 2020.
41. Rao VP and Epstein DL: Rho GTPase/Rho kinase inhibition as a novel target for the treatment of glaucoma. BioDrugs 21: 167-177, 2007.
42. Sharifi M, Nazarinia D, Ramezani F, Azizi Y, Naderi N and Aboutaleb N: Necroptosis and RhoA/ROCK pathways: Molecular targets of Nesfatin-1 in cardioprotection against myocardial ischemia/reperfusion injury in a rat model. Mol Biol Rep 48: 2507-2518, 2021.